

1 **Future anthropogenic land use change impacts on carbonaceous aerosol and implications
2 for climate and air quality**

3 Yang Shi¹, Colette L. Heald^{1,2}, Maria Val Martin³

4 ¹Civil and Environmental Engineering Department, Massachusetts Institute of Technology,
5 Cambridge, MA 02139, USA

6 ²Institute for Atmospheric and Climate Science, ETH Zurich, Zurich, 8092, Switzerland

7 ³School of Biosciences, University of Sheffield, Sheffield, S10 2TN, UK

8 *Correspondence to:* Yang Shi (yangshi@mit.edu) and Colette Heald (colette.heald@env.ethz.ch)

9

10 **Key words:**

11 Anthropogenic land use change; carbonaceous aerosol; fire; biogenic VOC; organic aerosol

12

13 **Key Points:**

14 • Future anthropogenic land use change (LUC) will perturb biogenic and fire emissions,
15 thereby modulating atmospheric carbonaceous aerosol.

16 • The predicted change in carbonaceous aerosol loading results in moderate future aerosol
17 direct radiative forcing.

18 • Anthropogenic LUC may be more important than anthropogenic emissions in
19 determining future carbonaceous aerosol burden.

20

21 **Abstract.**

22 Future anthropogenic land use change (LUC) may alter atmospheric carbonaceous aerosol (black
23 carbon and organic aerosol) burden by perturbing biogenic and fire emissions. However, there
24 has been little investigation of this effect. We examine the global
25 evolution of future carbonaceous aerosol under the Shared Socioeconomic Pathways projected
26 reforestation and deforestation scenarios using the CESM2 model from present-day to 2100.
27 Compared to present-day, the change in future biogenic volatile organic compounds emission
28 follows changes in forest coverage, while fire emissions decrease in both projections, driven by
29 trends in deforestation fires. The associated carbonaceous aerosol burden change produces
30 moderate aerosol direct radiative forcing (-0.021 to +0.034 W/m²) and modest mean reduction in
31 PM_{2.5} exposure (-0.11 µg/m³ to -0.23 µg/m³) in both scenarios. We find that future
32 anthropogenic LUC may be more important in determining atmospheric carbonaceous aerosol
33 burden than direct anthropogenic emissions, highlighting the importance of further constraining
34 the impact of LUC.

35

36 Plain Language Summary

37 Land is an important source for carbon-containing aerosols – fires emit soot and organics, while
38 forests emit organic gases that form organic aerosols through chemical reactions in the
39 atmosphere. Future anthropogenic activities, including reforestation and cropland expansion,
40 may change the land use type and thus perturb the carbon-containing aerosols in the atmosphere.
41 However, there has been little investigation on this topic. In this work, we study how the carbon-
42 containing aerosol may change from the present to the end of the century under projected
43 reforestation and deforestation pathways using a global climate model. We find that biogenic
44 emissions follow the forest coverage, and fire emissions decrease in both projections due to a
45 reduction in tropical anthropogenic deforestation by the end of the century. The resulting change
46 in carbon-containing aerosol moderately cool or warm the climate at the end of the century
47 because aerosols can scatter and/or absorb solar radiation. It also leads to a modest improvement
48 in global air quality. We highlight the importance of further constraining the impact of future
49 anthropogenic land use change, since we find that it may be even larger than the impact of
50 anthropogenic emissions on the loading of carbon-containing aerosols in the atmosphere.

51

52 **1 Introduction**

53 Carbonaceous aerosols, including organics (both primary, POA and secondary, SOA) and
54 black carbon (BC), make up 20% to 80% of the fine aerosol mass in the troposphere (Jimenez et
55 al., 2009; Zhang et al., 2007). These particles alter the Earth's climate directly through scattering
56 and absorbing radiation and indirectly through perturbing cloud properties (Chung & Seinfeld,
57 2002). They also contribute to surface fine particulate matter (PM_{2.5}, i.e., particulate matter with
58 diameter smaller than 2.5 micrometers), exposure to which is harmful for human health (Burnett
59 et al., 2018). It is therefore crucial to estimate how carbonaceous aerosol levels will evolve in a
60 future atmosphere.

61 Human activities have substantially altered global landscapes, converting 37% of land
62 area into cropland and grazing land (Klein Goldewijk et al., 2017). The terrestrial biosphere is an
63 important source of trace gases and aerosols, and thus anthropogenic land use change (LUC),
64 such as forestry management and agricultural development, may critically impact atmospheric
65 composition (Heald & Spracklen, 2015; Ward et al., 2014; Ward and Mahowald, 2015). This
66 represents an underexplored anthropogenic forcing on climate.

67 Changes to vegetation and fire activity associated with LUC can modulate the sources of
68 carbonaceous aerosol and its precursors. Natural vegetation produces biogenic volatile organic
69 compounds (BVOCs), which oxidize in the atmosphere to form lower volatility products which
70 can condense to form SOA (Hallquist et al., 2009). The emissions of BVOCs strongly depend on
71 the vegetation type. For example, broadleaf trees are stronger emitters than crops and grasses
72 (Guenther et al., 2012). Therefore, deforestation (reforestation) has been found to be associated
73 with decrease (increase) in biogenic SOA concentrations (Heald et al., 2008; Heald & Geddes,
74 2016; Unger, 2014; Weber et al., 2024). Wildfires emit BC, POA, and SOA precursors. LUC

75 influences fire emissions by altering the above-ground biomass and thus fuel availability (Kloster
76 et al., 2010, 2012) and through socio-economic changes linked to conversion between natural
77 and anthropogenic landscapes, such as savannah to cropland (Andela et al., 2017). In addition,
78 deforestation fires in the tropics are a critical and variable source of emissions (Li et al., 2018;
79 van der Werf et al., 2010), contributing ~ 20% of global carbon emissions in present day (PD)
80 (Li et al., 2013; van der Werf et al., 2010, 2017).

81 Anthropogenic LUC is projected to continue to the end of this century. Recent
82 predictions from the Shared Socioeconomic Pathways (SSPs) suggest that total cropland may
83 expand or contract in the future, accompanied by changes in forests and other natural lands
84 (Riahi et al., 2017). However, there has been little exploration of how future LUC itself will
85 impact carbonaceous aerosols and the attendant climate forcing and air quality. Previous studies
86 suggested that anthropogenic LUC will alter the SOA burden by -20% to 30% by 2100 from PD
87 (Heald et al., 2008; Lund et al., 2021; Wu et al., 2012; Scott et al., 2018; Ward et al., 2014). But
88 these studies either used LUC from old scenarios that only consider deforestation or applied
89 idealized land use perturbations. Kloster et al. (2012) tested different Representative
90 Concentration Pathway (RCP) scenarios and estimated that projected LUC and wood harvest
91 would decrease total fire carbon emissions by 5 to 35%, but they did not extend their results to
92 atmospheric aerosols. Ward et al. (2014) found that LUC could modify fire aerosol emissions by
93 -21% to 21% from 2010 to 2100, depending on RCP trajectories. However, the radiative forcings
94 associated with these LUC-driven fire aerosol changes were not estimated.

95 **2 Methods**96 **2.1 CLM5 and CAM6-Chem**

97 We use the land and atmosphere components of the Community Earth System Model
98 version 2.2 (CESM2.2; Danabasoglu et al., 2020) – Community Land Model version 5 (CLM5;
99 Lawrence et al., 2019) and Community Atmosphere Model version 6 with chemistry (CAM6-
100 Chem; Emmons et al., 2020).

101 The active biogeochemistry configuration of the CLM5 model used here prognostically
102 calculates leaf area index (LAI). It includes 16 natural plant functional types and 8 active crops,
103 which we grouped into seven land use types (i.e., tropical, temperate, and boreal tree, grass,
104 shrub, crop, and bare soil) in the analysis for simplicity. BVOC emissions respond to light,
105 temperature, leaf age, and CO₂ following the Model of Emissions of Gases and Aerosols from
106 Nature (MEGAN) version 2.1 (Guenther et al., 2012). A prognostic fire model predicts smoke
107 emissions (Li et al., 2012, 2013; Li & Lawrence, 2017), accounting for four types of fires:
108 agricultural fires in cropland, deforestation fires in tropical closed forest, non-peat fires outside
109 cropland and tropical closed forest, and peat fires. Fire burned area is determined by climate
110 factors, vegetation properties, and human activities. The deforestation fire burned area is also
111 related to the annual loss of tropical tree cover at each grid cell. Fire carbon emissions are
112 estimated considering burned area and surface carbon density; emissions of trace gases and
113 aerosol species are scaled from the fire carbon emissions using emission factors, which are
114 dependent on the vegetation type. Peat fire emissions are unaffected by LUC and thus excluded
115 from our analyses below (Figure S1). This fire model has been extensively evaluated and widely
116 used by previous studies (see Texts S1.1 and S1.2), but we note that further work is needed to

117 evaluate how well the model responds to LUC perturbations. Species emitted from biogenic and
118 fire sources are tabulated in Table S1.

119 The CAM6-Chem model includes the MOZART-TS1 chemistry (Model of Ozone and
120 Related chemical Tracers with tropospheric and stratospheric chemistry; Emmons et al., 2020)
121 and a 4-mode version of the modal aerosol model (MAM4; Text S2 and Liu et al., 2016). Three
122 carbonaceous aerosols (i.e., BC, POA, and SOA) are represented in MAM4. BC and POA are
123 emitted from both fire and anthropogenic sources. All the fire emissions are injected into the
124 model surface layer without considering the plume injection height (Val Martin et al., 2010),
125 which is highly uncertain; previous studies disagree on the importance of this factor (Carter et al.,
126 2020; Lu et al., 2024; Tang et al., 2022; Veira et al., 2015). SOA formation from the oxidation of
127 VOCs is parameterized through the volatility basis set that considers NO_x-dependent yields
128 (Hodzic et al., 2016; Jo et al., 2021; Tilmes et al., 2019). VOCs precursors for SOA formation
129 are also shown in Table S1.

130 **2.2 Experiments**

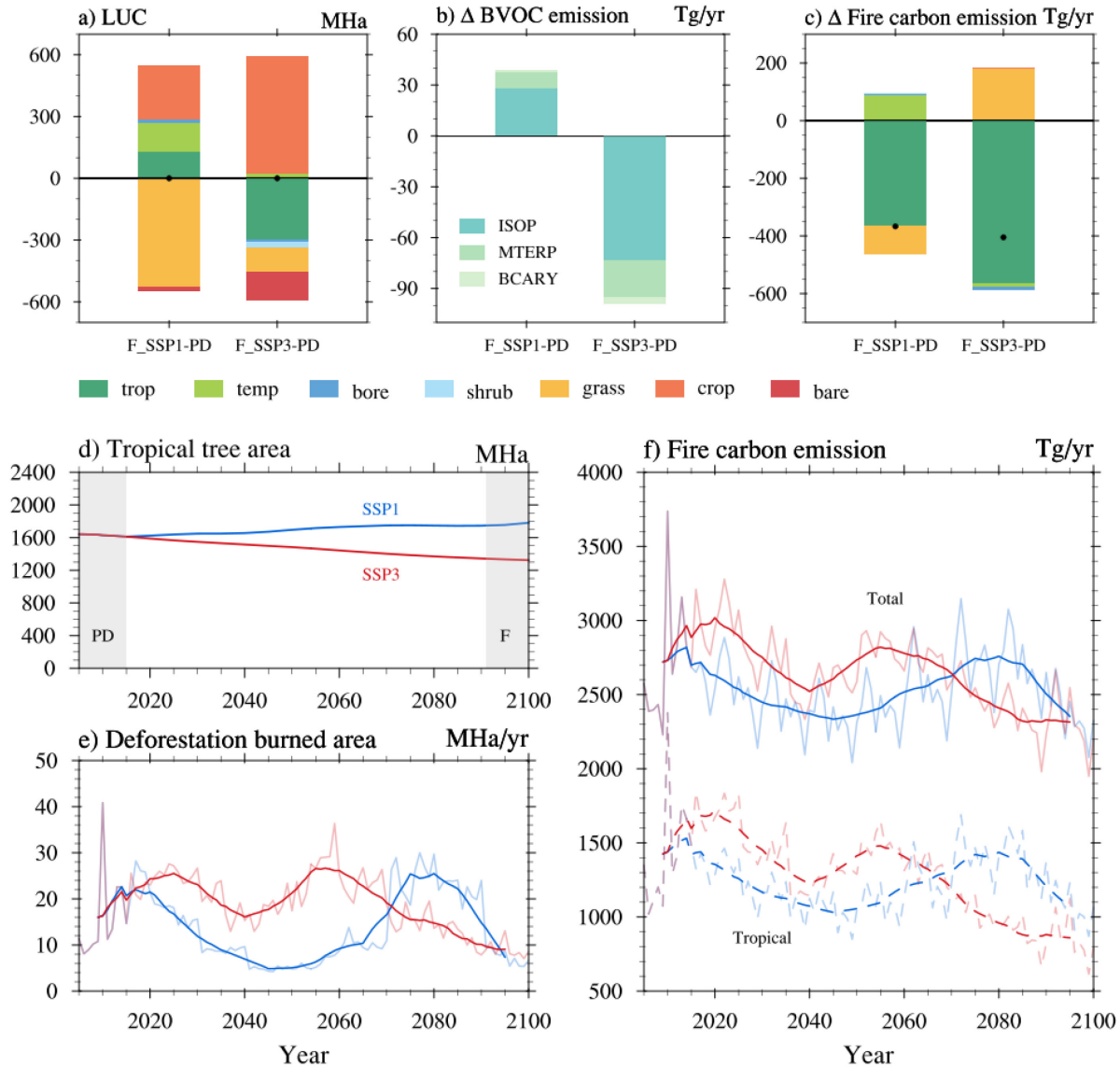
131 We conducted model experiments in two steps: (1) estimating biogenic and fire emissions
132 with evolving anthropogenic LUC using CLM5 and then (2) exploring the climate and the air
133 quality impacts of the LUC-driven carbonaceous aerosol changes using CAM6-Chem.

134 For the first step, two CLM5 experiments were conducted using land use data following
135 the SSP1-2.6 and SSP3-7.0 pathways (hereafter SSP1 and SSP3; Riahi et al., 2017). These two
136 pathways are chosen because they bracket the range of projected global reforestation (SSP1) and
137 deforestation (SSP3). But we note that in SSP1 (SSP3) there may be local deforestation
138 (reforestation) (Figure S2). Initially, we spun up CLM5 to steady state in 1850 for about 1200
139 years to reach equilibrium. Subsequently, a spin-up from 1850 to 2004 was conducted using

140 historical data. The two future simulations were run from 2005 to 2100, with meteorology
141 cycling from 2001 to 2010 following offline dataset, CO₂ concentrations fixed to year 2005, and
142 population density fixed to year 2010. Simulated biogenic and fire emissions were averaged over
143 the first (2005-2014) and last (2091-2100) ten years of the simulations to generate
144 climatologically monthly emission files for PD and future (F) conditions. We note that both
145 SSP1 and SSP3 simulations have the same PD emissions because the land use data are identical
146 before 2015. The annual total fire carbon emission for PD (2720 Tg/yr) falls within the range of
147 Global Fire Emission Database version 4.1s (GFED4.1s; 2027 Tg/yr; Randerson et al., 2018) and
148 Fire Inventory from NCAR version 2.5 (FINNv2.5; 3399 Tg/yr; Wiedinmyer et al., 2023) over
149 the same years with few regional exceptions (Table S2; see Figure S3 and Text S1.3 for
150 comparisons in spatial patterns), which indicates a reasonable representation of the fire emission
151 in the CLM5 fire model.

152 For the second step, we performed three CAM6-Chem experiments (one PD and two F)
153 driven by the biogenic and fire emissions generated from the CLM5 experiments. Anthropogenic
154 emissions were set to PD climatology (Hoesly et al., 2018) in all the three experiments. By
155 comparing the two F experiments with the PD experiment, we estimate the climate and air
156 quality impacts of LUC-driven carbonaceous aerosol change. In addition, to investigate the
157 relative importance of LUC and anthropogenic emissions, another two CAM6-Chem
158 experiments were conducted using future SSP1-2.6 and SSP3-7.0 anthropogenic emissions
159 (Riahi et al., 2017) but keeping biogenic and fire emissions and climate at PD (see Section 3.4).
160 Anthropogenic emissions related to carbonaceous aerosols include those for BC, POA, and
161 anthropogenic VOCs (Table S1). All simulations were performed for 11 years with the first year
162 used for spin-up at 0.9° × 1.25° horizontal resolution and 32 vertical layers.

163 In each CAM6-Chem experiment, we added diagnostic radiative calls that remove total
164 carbonaceous aerosol and each carbonaceous aerosol species, respectively, to estimate the
165 effective radiative forcing due to aerosol-radiation interaction (ERF_{ari} ; also known as direct
166 radiative forcing) from PD to F. We first calculated the direct radiative effects by taking the
167 difference between default radiative fluxes and those from diagnostic calls that remove
168 corresponding aerosol species. Then, the ERF_{ari} was defined as the direct radiative effect in F
169 with respect to PD. We note that we do not account for the radiative forcing related to aerosol-
170 cloud interactions (i.e., indirect forcing).

171 **3 Result**172 **3.1 Emissions response to LUC**

173

174 **Figure 1.** a) LUC b) BVOC (ISOP: isoprene, MTERP: monoterpane, and BCARY:
 175 sesquiterpene) emission change, and c) total fire carbon emission change from PD to F projected
 176 by SSP1 and SSP3. LUC and fire carbon emission change are shown in land use classes (trop:
 177 tropical tree, temp: temperate tree, bore: boreal tree, shrub, grass, crop, and bare: bare soil) and

178 categorized by colors. Black dots on panel a) and c) are global total changes. Panels d-f show
179 SSP1 (blue lines) and SSP3 (red lines) projections of tropical tree area, deforestation burned area,
180 and fire carbon emission, respectively. Gray shading on panel d) marks the time periods treated
181 as PD (2005-2014) and F (2091-2100). Light red and blue lines on panel e) and f) are yearly time
182 series, while darker lines are ten year running means. On panel f), solid and dashed lines are total
183 fire carbon emission and that from tropical tree, respectively. Figure S4 reproduces this figure in
184 a color-blind friendly version.

185

186 We first explore the LUC from PD to F as well as the corresponding changes in BVOC
187 and fire emissions using the CLM5 simulations (Figure 1a-c). The SSP1 scenario projects
188 reforestation over tropical and temperate forest accompanied by cropland expansion at the
189 expense of grassland (Figure 1a). Tropical reforestation is predominantly concentrated in Eastern
190 Brazil and tropical Africa except the Congo Basin, while temperate tree reforestation occurs in
191 the Eastern US, Europe, and Eastern China (Figure S2a-b). In contrast, SSP3 forecasts a
192 deforestation of tropical trees, primarily in tropical Africa and the western Amazon Forest
193 (Figure S2h), along with a moderate global reduction in grassland and bare soil and a substantial
194 increase in cropland (Figure 1a). We observe that, in SSP3, the change in grassland area is not
195 globally uniform – in particular, the African grassland change exhibits a dipole feature,
196 characterized by a significant increase in the Congo Rainforest and the Sahel but a decrease
197 elsewhere (Figure S2l).

198 The global total emissions for BVOCs, BC, and POA in PD and F are shown in Table S3.
199 In response to the reforestation in SSP1 and the deforestation in SSP3, total BVOC emissions,
200 including isoprene, monoterpenes, and sesquiterpenes, increase by 39 Tg/yr (5.6%) and

201 decreases by 99.3 Tg/yr (14.2%) in SSP1 and SSP3, respectively (Figure 1b). The percentage
202 change is consistent among the three classe(Hodzic et al., 2016)s of biogenic VOCs. The spatial
203 distribution of the change in BVOC emissions is generally positively correlated with the
204 alteration of tree coverage (Figures S2 and S5). In the SSP1 scenario, emissions increase in
205 Eastern US, Southern Africa, Europe, and Eastern China. The Amazon forest also shows slight
206 BVOC emissions increase (mostly < 2%) but has little LUC, which is related to LAI increases
207 (Figure S6). In the SSP3 scenario, the emissions decrease in the Southern Hemisphere (SH;
208 South America and Africa), India, Southeast Asia, and the East Coast of the US, whereas
209 emissions increase in the Midwest and South US, Europe, and Eastern China.

210 The total fire carbon emissions decrease by 367 Tg/yr in SSP1 and by 404.8 Tg/yr in
211 SSP3 (Figure 1c). This converts to a BC emission decrease of 0.4 TgC/yr (3.7%) in both F
212 projections and a POA emission decrease of 3.4 TgC/yr (5.6%) and 5.5 TgC/yr (9.1%) in SSP1
213 and SSP3, respectively (Table S3). The fire carbon emissions decrease is dominated by tropical
214 forest in both projections, despite the opposite changes in tropical forest extent (Figure 1c-d).
215 The fire emissions decrease in SSP1 (reforestation scenario) reflects the decrease in tropical
216 deforestation fires, outweighing the growth in fuel availability caused by tropical reforestation
217 (Figure 1e-f). Although global tropical tree coverage increases persistently in SSP1, regional
218 tropical tree loss exists, peaking around 2080 (Figure S7). In SSP3 (deforestation scenario), the
219 tropical tree loss and associated deforestation fires is stronger in the first half of the century,
220 peaking around 2020 and 2055. In the latter half of the century, deforestation fires decline and
221 the overall reduction in forest biomass over the tropics generate less fire carbon loss. Thus, the
222 total F (2091-2100) fire emissions are less than in PD. Our results indicate that around half of the
223 emissions originate from tropical forests (Figure 1f). This may be an overprediction, because

224 GFED4.1s suggests that tropical savannas account for 62% of total fire carbon emissions (van
225 der Werf et al., 2017). But it is worthwhile to note that satellite-based fire emission products also
226 rely on uncertain factors, like biogeochemical models, land cover datasets, and emission factors.
227 In addition, in the SSP3 projection, the global fire carbon emission from grassland increases
228 despite the global grassland coverage decreases (Figure 1a and 1c). This reflects the
229 heterogeneous response of fire carbon emission to LUC over grassland, which is related to
230 vegetation density (Figure S8).

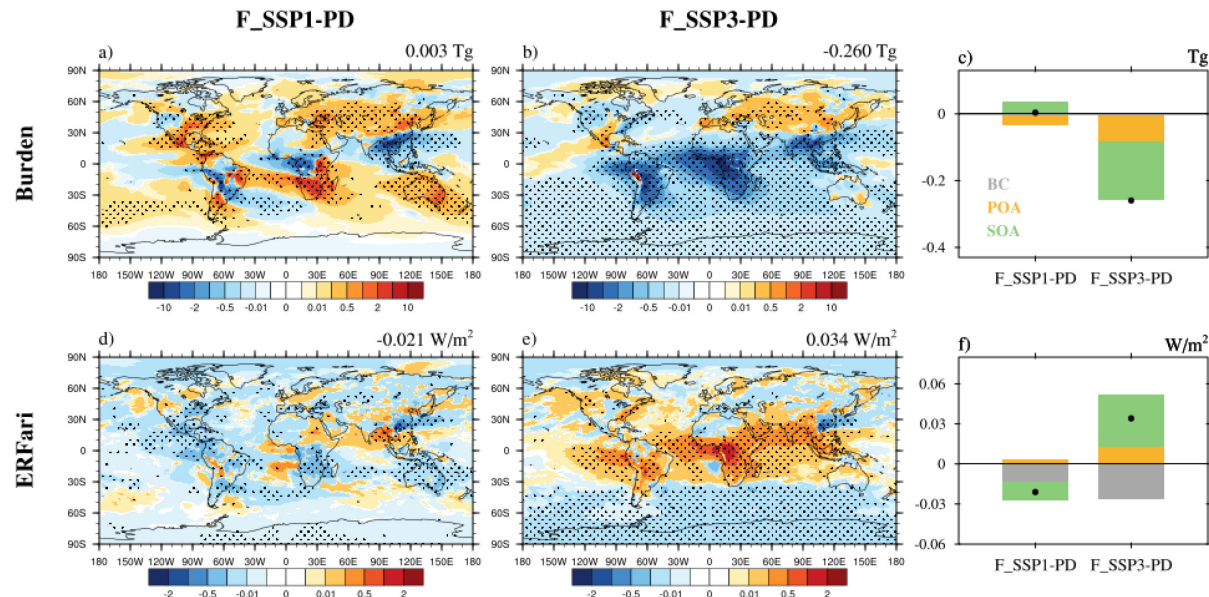
231 The fire emissions projected with the SSP1 LUC scenario show declines in the tropics but
232 growth in subtropics and the mid-latitudes (Figure S9). In SSP3, the fire emissions are projected
233 to mostly decrease in the tropics and the SH (Figure S9), in response to the tropical deforestation
234 and grassland shrink. However, there is an emission increase in the Congo Basin, which is the
235 combined result of both deforestation fire and grassland coverage increase. The conversion from
236 grassland into cropland decreases local fire emissions over South Africa and India in SSP3 (Text
237 S1.4). We note that the LUC in the Eastern US, Europe, and Eastern and Southern China are
238 relatively strong in both predictions but the changes in fire emission are minor, which reflects the
239 suppression of fire in these highly populated regions (Text S1.5). Also, both scenarios show
240 emission perturbations in East Siberia (in total, less than 2 Tg/yr) that may be related to
241 disturbance in soil moisture and other factors rather than LUC.

242 **3.2 Carbonaceous aerosol burden change and climate forcing**

243 In the SSP1, the global carbonaceous aerosol burden increases marginally by 0.003 Tg
244 (0.15%), which results from an increase in SOA (0.038 Tg; 4.4%), driven by biogenic emission
245 increases, mostly compensated by decreases in the fire-driven BC (-0.005 Tg; -3.9%) and POA (-
246 0.03 Tg; -3.9%) (Figure 2c). In the SSP3, the burden of all the three aerosol species decreases

247 (SOA: -0.175 Tg, -20.2%; BC: -0.006 Tg, -4.7%; POA: -0.079 Tg, -10.2%), following the
 248 decreases in both biogenic and fire emissions (Figures 2c). This leads to a substantial total
 249 carbonaceous aerosol burden decrease (-0.26 Tg, -12.6%). The two scenarios result in
 250 particularly different trajectories over the SH (Figure 2a-b) – the carbonaceous aerosol burden
 251 decreases significantly and consistently in the SH in SSP3, whereas in SSP1, the change is
 252 largely positive. Given the relatively short lifetime of aerosols, the spatial distribution of the
 253 burden change generally follows local emission changes (Figure S10a-f). We notice that the
 254 aerosol lifetime changes slightly from PD to F due to changing geographical distribution of
 255 emissions (Table S4).

256



257

258 **Figure 2.** Annual change in total carbonaceous aerosol burden (top row; unit: mg/m^2) and the
 259 ERF_{ari} from PD to future (bottom row; unit: W/m^2). Dotted regions on panel a-b and d-e are
 260 where the changes are significant to the 0.05 levels. Numbers on the top right of each panel are
 261 global total burden (a-b) and global average ERF_{ari} (d-e). Also shown are global total burden (c)

262 and global averaged ERF_{ari} (f) with contribution from individual aerosol species classified by
263 colors. Black dots on the two panels (c and f) are changes in total carbonaceous aerosols.

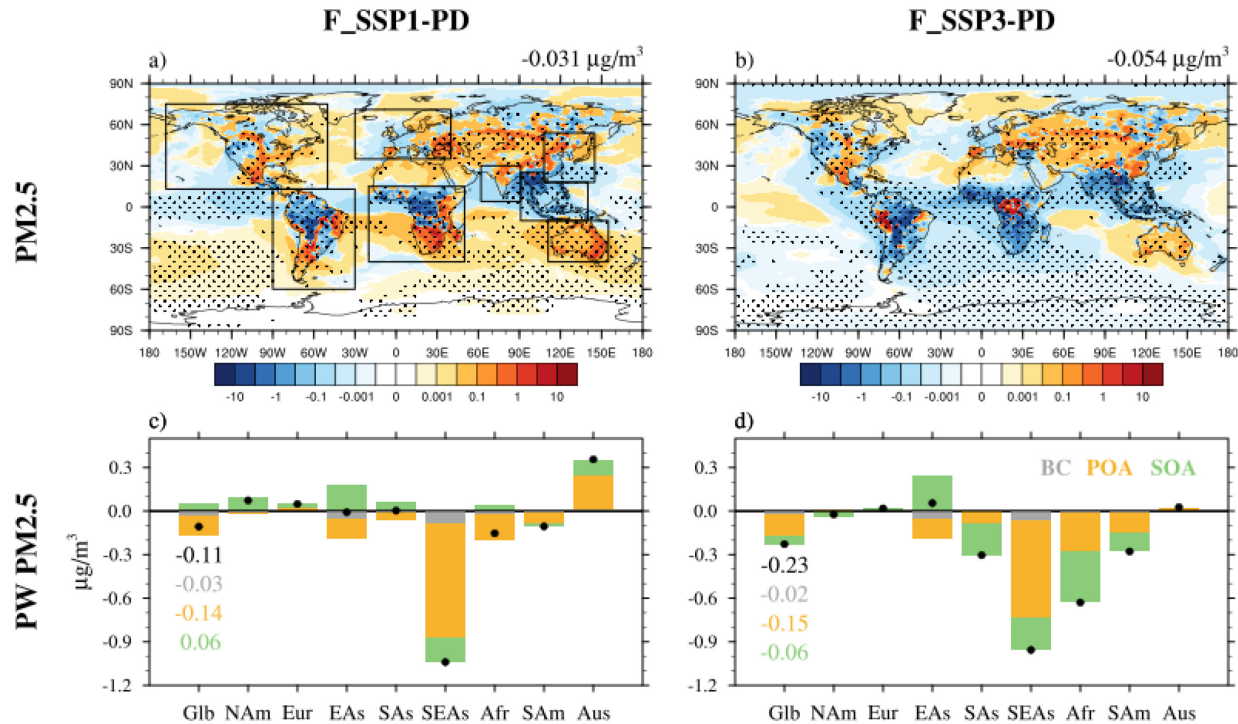
264

265 Carbonaceous aerosols impact the climate through direct interactions with shortwave
266 radiation – POA and SOA have net cooling radiative effect through scattering shortwave
267 radiation, while BC is a light-absorbing aerosol that has a strong warming effect. We note here
268 that given uncertainties in the sources and photochemical evolution of brown carbon, we neglect
269 the warming effect of this contribution to POA and SOA. This may be somewhat compensated
270 by fire aerosols that are too strongly absorbing (Brown et al., 2021). For SSP1, the global
271 averaged ERF_{ari} due to LUC-driven total carbonaceous aerosol change is -0.021 W/m^2 (Figure
272 2d), which is dominated by a cooling due to the BC burden decrease and the SOA burden
273 increase that overweighs the warming caused by the POA burden decrease (Figure 2f). In SSP3,
274 the decrease in POA and SOA burden results in a strong warming ERF_{ari} whereas there is a
275 moderate cooling caused by BC burden decrease. As a result, the global ERF_{ari} for total
276 carbonaceous aerosol is $+0.034 \text{ W/m}^2$ in SSP3. The warming predominantly occurs over the
277 tropical and subtropical regions in the SH, with regional forcing that exceeds 0.1 W/m^2 . We note
278 that the decreasing aerosol burden at mid and high southern latitudes leads to a cooling due to
279 preponderance of POA and SOA above cloud during the poleward transport in the SH. Overall,
280 the future LUC-driven ERF_{ari} of the carbonaceous aerosol in both projections are on the order of
281 $\sim 10\%$ of the total aerosol ERF_{ari} ($-0.3 \pm 0.3 \text{ W/m}^2$) from 1750 to 2014 estimated by IPCC AR6
282 (Forster et al., 2021).

283 We find that SOA has the largest burden change among the three aerosol species in both
284 future predictions. Moreover, the ERF_{ari} from the fire aerosols (i.e., BC and POA) oppose each

285 other and produce a forcing that is smaller in magnitude compared to that of SOA. Therefore, we
 286 conclude that the LUC-driven biogenic emissions have larger impact on carbonaceous aerosol
 287 burden and climate forcing than the LUC-driven fire emissions in these simulations.

288 **3.3 Surface PM_{2.5}**



289

290 **Figure 3.** Top row: same as panel a) and b) in Figure 2, except for total carbonaceous aerosol
 291 PM_{2.5} surface concentrations. Global (Glb) and regional (NAm: North America, Eur: Europe,
 292 EAs: East Asia, SAs: South Asia, SEAs: Southeast Asia, Afr: Africa, SAM: South America, Aus:
 293 Australia) average surface population weighted (PW) PM_{2.5} concentrations are shown on the
 294 bottom panels. Borders of regions are shown by black rectangles in panel a). Contributions from
 295 individual species are classified by different colors, while the black dots represent total changes.
 296 Global averaged total PW PM_{2.5} concentrations are given in black numbers, with contribution
 297 from each aerosol species shown by numbers in corresponding colors.

298

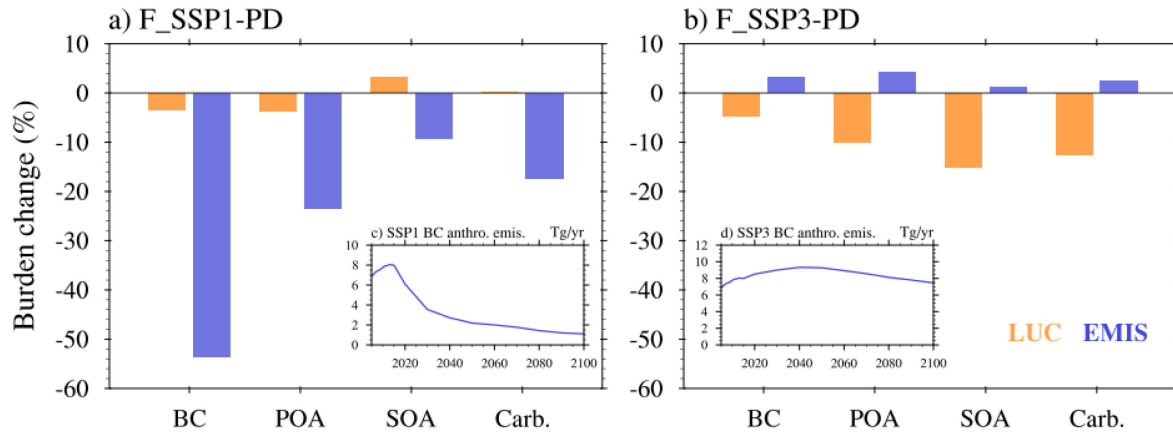
299 LUC-driven changes in carbonaceous aerosol, which contribute to surface PM_{2.5}, have
300 implications for human health. Figure 3a-b shows the global distributions of surface
301 carbonaceous aerosol PM_{2.5} concentration change from PD to F. In contrast to the burden
302 increase, global averaged surface PM_{2.5} concentrations decrease by -0.031 µg/m³ (-5.1%) in the
303 SSP1 projection. This difference is due to the change in SOA, whose global burden increases
304 (Figure S10c) but surface concentration slightly decreases (Figure S11c). The strongest decrease
305 occurs over the tropics, including the Amazon Forest, mid-Africa, and Southeast Asia. These
306 regions have dense forest and therefore large BVOC emissions (Guenther et al., 2012). As a
307 result, surface OH is depleted and the SOA formation timescale is extended, making surface
308 SOA levels rather insensitive to VOC emission increases. Instead, the fire-driven decrease in
309 POA concentration has a larger impact on SOA by limiting the condensation of precursor gases.
310 Therefore, the change in surface SOA concentration mostly follows the POA change in the
311 tropics (Figure S11b-c). In the SSP3 projection, the surface total PM_{2.5} concentration decreases
312 by -0.054 µg/m³ (-8.9%), because of reductions in all three aerosol species. The change in
313 surface SOA is due to changes in both BVOC emissions and surface POA concentrations.

314 To estimate the impact of the change in carbonaceous aerosols on human PM_{2.5} exposure,
315 we calculate the global and regional population weighted (PW) PM_{2.5} changes (Figure 3c-d). We
316 use 2010 from the Gridded Population of the World, Version 4 dataset (SEDAC, 2018) for both
317 PD and F. Globally, the total surface PW PM_{2.5} concentration decreases in both SSP1 (by -0.11
318 µg/m³) and SSP3 (by -0.23 µg/m³). The reduction in both projections is dominated by the change
319 in POA concentrations driven by decreases in fire emission. The global averaged improvement in
320 air quality in both projections is modest comparing to the World Health Organization air quality

321 guideline level ($5 \mu\text{g}/\text{m}^3$; WHO, 2021), with larger regional improvements (e.g. nearly $1 \mu\text{g}/\text{m}^3$
 322 over Southeast Asia).

323 Globally, the fire aerosols drive the reductions in PW PM_{2.5} surface concentrations, both
 324 directly and via changing the partitioning of SOA. Therefore, from our simulations we conclude
 325 that the air quality response to anthropogenic LUC is dominated by the trajectory of fire
 326 emissions. We note that our conclusions here and in Section 3.2 are both subjected to
 327 uncertainties related to fire plume injection heights – injecting smoke emissions aloft will reduce
 328 the LUC-driven fire PW PM_{2.5} decrease at the surface and may impact aerosol transport and
 329 climate radiative effects (See Figure S12 and Text S3).

330 **3.4 Relative importance of LUC and anthropogenic emissions changes**



331
 332 **Figure 4.** Percentage change in atmospheric carbonaceous aerosol burden in the two future
 333 scenarios compared with PD, for a) F_SSP1 and b) F_SSP3. Bars represent the impact of
 334 anthropogenic LUC (orange) and anthropogenic emission (EMIS, blue) changes. Inset panels are
 335 time series for anthropogenic BC emissions following c) SSP1 and d) SSP3.

336

337 Anthropogenic emissions of carbonaceous aerosol are projected to change in the next
338 century in response to socio-economic factors, including air quality regulation. The SSP1 is a
339 strong pollution control scenario, which exhibits a rapid decline globally in anthropogenic
340 emissions (Figures 4c and S13-S14). In contrast, the SSP3 scenario assumes that the
341 implementation of pollution controls is delayed. Therefore, anthropogenic emissions increase
342 slightly over the short-term, except over developed regions, and declines in the second half of the
343 century when strong emission reductions also occur in Asia (Figure S13). As a result, the end of
344 century emissions in SSP3 are comparable to the level at PD (Figures 4d and S14).

345 Figure 4 compares the percentage change in atmospheric carbonaceous aerosol burden
346 due to anthropogenic LUC and anthropogenic emissions change. In the SSP1 projection, the
347 reduction in anthropogenic emissions has a more substantial impact on carbonaceous aerosol
348 burden than LUC. In contrast, the LUC-driven emission change plays a more important role in
349 the SSP3 projection. Therefore, depending on which pathway we take, the impact of
350 anthropogenic LUC may outweigh the impact of anthropogenic emission changes on the
351 abundance of carbonaceous aerosol and, consequently, the climate forcing and air quality.

352 Previous studies suggest that climate change will increase future atmospheric
353 carbonaceous aerosols (Heald et al., 2008; Kloster et al., 2012; Sporre et al., 2019). We
354 conducted two additional CLM5 experiments and find that the magnitude of emission changes
355 due to LUC is 25-128% of that due to climate change (Figure S15 and Text S4), highlighting that
356 both climate change and LUC have a substantial impact on carbonaceous aerosol sources.

357 **4. Conclusions**

358 In this study, we investigate the response of carbonaceous aerosols (i.e., BC, POA, and
359 SOA) to future anthropogenic LUC using CESM2. We test two future LUC projections (SSP1-
360 2.6 and SSP3-7.0), which bracket the range of reforestation and deforestation. In response to the
361 forest coverage change, BVOC emissions increase in SSP1 and decrease in SSP3. However, fire
362 emission decrease in both projections. Dynamically varying tropical fires dominate the fire
363 emission trends. Therefore, the fire emissions do not monotonically follow LUC, which
364 emphasizes that the time horizon selected to quantify the effect of LUC is critical. We find that
365 the LUC-driven carbonaceous aerosol emission change by end of century results in a direct
366 radiative forcing that is cooling in SSP1 and warming in SSP3, the magnitude of which are
367 moderate as compared to the total historical ERF_{ari} for aerosol in IPCC AR6. Both future LUC
368 scenarios result in modest improvements in air quality. Overall, with the two future pathways
369 tested in this study, we conclude that the LUC-driven biogenic emissions may have a larger
370 impact on climate forcing, while the LUC-driven fire emissions may be more important for air
371 quality. We note that our study relies on existing land (including fire parameterizations and their
372 relationship to land use change) and atmospheric models and commonly used SSP projections,
373 all of which introduce uncertainties to our results. Given that we find that LUC represents a
374 considerable perturbation to future carbonaceous aerosol concentrations, future research is
375 needed to improve these model schemes and datasets to reduce the associated uncertainties.

376 Biogenic and fire aerosols are generally overlooked when quantifying aerosol climate
377 forcing (e.g., in IPCC AR6 and the modeling studies it builds upon). Our work demonstrates that
378 LUC is an anthropogenic mechanism that can alter these aerosols, regardless of whether their
379 source is natural or anthropogenic. We find that this pathway may be an even more important

380 driver than direct anthropogenic emissions in modifying atmospheric carbonaceous aerosol
381 burden and thus in determining the future climate forcing and air quality impact of carbonaceous
382 aerosols. This highlights the importance of including these effects in future climate simulations
383 and improving our understanding of how fire and biogenic emissions respond to changing land
384 use as well as climate.

385 **Acknowledgements**

386 This work was supported by the U.S. National Science Foundation (AGS-2223070) and
387 Department of Energy (DE-SC0022017). MVM is supported by the UKRI Future Leaders
388 Fellowship Programme (MR/T019867/1). We gratefully acknowledge high-performance
389 computing support from Cheyenne (doi:10.5065/D6RX99HX) provided by NCAR's
390 Computational and Information Systems Laboratory, sponsored by the National Science
391 Foundation.

392 **Open Research**

393 Datasets used for model evaluation include the GFED4.1 fire emission data (Randerson
394 et al., 2018), the FINNv2.5 fire emission data (Wiedinmyer et al., 2023), and the global
395 population dataset (SEDAC, 2018). This work is based on CESM2.2 (NCAR, 2023). The data
396 shown in the figures is available on Zenodo (Shi et al., 2025).

397 **References**

398 Andela, N., Morton, D. C., Giglio, L., Chen, Y., van der Werf, G. R., Kasibhatla, P. S., et al.
399 (2017). A human-driven decline in global burned area. *Science*, 356, 1356-1362.
400 <https://doi.org/10.1126/science.aal4108>

401 Andela, N., & van der Werf, G. R. (2014). Recent trends in African fires driven by cropland
402 expansion and El Niño to La Niña transition. *Nature Climate Change*, 4, 791-795.
403 <https://doi.org/10.1038/NCLIMATE2313>

404 Aragão, L. E. O. C., Malhi, Y., Barbier, N., Lima, A., Shimabukuro, Y., Anderson, L., &
405 Saatchi, S. (2008). Interactions between rainfall, deforestation and fires during recent
406 years in the Brazilian Amazonia. *Philosophical Transactions of the Royal Society B:
407 Biological Sciences*, 363(1498), 1779–1785. <https://doi.org/10.1098/rstb.2007.0026>

408 Brown, H., Liu, X., Pokhrel, R., Murphy, S., Lu, Z., Saleh, R., et al. (2021). Biomass burning
409 aerosols in most climate models are too absorbing. *Nature Communications*, 12, 277,
410 <https://doi.org/10.1038/s41467-020-20482-9>

411 Burnett, R., Chen, H., Szyszkowicz, M., Fann, N., Hubbell, B., Pope, C. A., et al. (2018). Global
412 estimates of mortality associated with long-term exposure to outdoor fine particulate
413 matter. *Proceedings of the National Academy of Sciences*, 115(38), 9592–9597.
414 <https://doi.org/10.1073/pnas.1803222115>

415 Butt, E. W., Conibear, L., Smith, C., Baker, J. C. A., Rigby, R., Knote, C., & Spracklen, D. V.
416 (2022). Achieving Brazil's Deforestation Target Will Reduce Fire and Deliver Air
417 Quality and Public Health Benefits. *Earth's Future*, 10(12), e2022EF003048.
418 <https://doi.org/10.1029/2022EF003048>

419 Chen, Y., Hall, J., van Wees, D., Andela, N., Hantson, S., Giglio, L., et al. (2023). Multi-decadal
420 trends and variability in burned area from the fifth version of the Global Fire Emissions
421 Database (GFED5). *Earth System Science Data*, 15, 5227-5259.
422 <https://doi.org/10.5194/essd-15-5227-2023>

423 Chung, S. H. & Seinfeld. (2002). Global distribution and climate forcing of carbonaceous
424 aerosols. *Journal of Geophysical Research*, 107(D19), 4407.
425 <https://doi.org/10.1029/2001JD001397>

426 Danabasoglu, G., Lamarque, J.-F., Bacmeister, J., Bailey, D. A., DuVivier, A. K., Edwards, J., et
427 al. (2020). The Community Earth System Model Version 2 (CESM2). *Journal of*
428 *Advances in Modeling Earth Systems*, 12(2), e2019MS001916.
429 <https://doi.org/10.1029/2019MS001916>

430 Emmons, L. K., Schwantes, R. H., Orlando, J. J., Tyndall, G., Kinnison, D., Lamarque, J., et al.
431 (2020). The Chemistry Mechanism in the Community Earth System Model Version 2
432 (CESM2). *Journal of Advances in Modeling Earth Systems*, 12(4).
433 <https://doi.org/10.1029/2019MS001882>

434 Fischer, E. V., Jacob, D. J., Yantosca, R. M., Sulprizio, M. P., Millet, D. B., Mao, J., et al.
435 (2014). Atmospheric peroxyacetyl nitrate (PAN): a global budget and source attribution.
436 *Atmospheric Chemistry and Physics*, 14, 2679-2698. <https://doi.org/10.5194/acp-14-2679-2014>

438 Forster, P., Storelvmo, T., Armour, K., Collins, W., Dufresne, J.-L., Frame, D., et al. (2021): The
439 Earth's Energy Budget, Climate Feedbacks, and Climate Sensitivity. In V. P. Masson-
440 Delmotte et al. (Eds.), *Climate Change 2021: The Physical Science Basis. Contribution of*
441 *Working Group I to the Sixth Assessment Report of the Intergovernmental Panel on*

442 Climate Change (pp. 923-1054). Cambridge, United Kingdom and New York, NY, USA:
443 Cambridge University Press. <https://doi.org/10.1017/9781009157896>

444 Guenther, A. B., Jiang, X., Heald, C. L., Sakulyanontvittaya, T., Duhl, T., Emmons, L. K., &
445 Wang, X. (2012). The Model of Emissions of Gases and Aerosols from Nature version
446 2.1 (MEGAN2.1): an extended and updated framework for modeling biogenic emissions.
447 *Geoscientific Model Development*, 5(6), 1471–1492. <https://doi.org/10.5194/gmd-5-1471-2012>

449 Hallquist, M., Wenger, J. C., Baltensperger, U., Rudich, Y., Simpson, D., Claeys, M., et al.
450 (2009). The formation, properties and impact of secondary organic aerosol: current and
451 emerging issues. *Atmospheric Chemistry and Physics*, 9(14), 5155–5236.
452 <https://doi.org/10.5194/acp-9-5155-2009>

453 Hantson, S., Kelley, D. I., Arneth, A., Harrison, S. P., Archibald, S., Bachelet, D., et al. (2020).
454 Quantitative assessment of fire and vegetation properties in simulations with fire-enabled
455 vegetation models from the Fire Model Intercomparison Project. *Geoscientific Model
456 Development*, 13(7), 3299–3318. <https://doi.org/10.5194/gmd-13-3299-2020>

457 Heald, C. L., Henze, D. K., Horowitz, L. W., Feddema, J., Lamarque, J.-F., Guenther, A., et al.
458 (2008). Predicted change in global secondary organic aerosol concentrations in response
459 to future climate, emissions, and land use change: FUTURE PREDICTED CHANGE IN
460 GLOBAL SOA. *Journal of Geophysical Research: Atmospheres*, 113(D5), n/a-n/a.
461 <https://doi.org/10.1029/2007JD009092>

462 Heald, C. L., & Geddes, J. A. (2016). The impact of historical land use change from 1850 to
463 2000 on secondary particulate matter and ozone. *Atmospheric Chemistry and Physics*,
464 16(23), 14997–15010. <https://doi.org/10.5194/acp-16-14997-2016>

465 Heald, C. L., & Spracklen, D. V. (2015). Land Use Change Impacts on Air Quality and Climate.

466 *Chemical Reviews*, 115(10), 4476–4496. <https://doi.org/10.1021/cr500446g>

467 Hodzic, A., Kasibhatla, P. S., Jo, D. S., Cappa, C. D., Jimenez, J. L., Madronich, S., & Park, R. J.

468 (2016). Rethinking the global secondary organic aerosol (SOA) budget: stronger

469 production, faster removal, shorter lifetime. *Atmospheric Chemistry and Physics*, 16(12),

470 7917–7941. <https://doi.org/10.5194/acp-16-7917-2016>

471 Hoesly, R. M., Smith, S. J., Feng, L., Klimont, Z., Janssens-Maenhout, G., Pitkanen, T., et al.

472 (2018). Historical (1750–2014) anthropogenic emissions of reactive gases and aerosols

473 from the Community Emissions Data System (CEDS). *Geoscientific Model Development*,

474 11(1), 369–408. <https://doi.org/10.5194/gmd-11-369-2018>

475 Jimenez, J. L., Canagaratna, M. R., Donahue, N. M., Prevot, A. S. H., Zhang, Q., Kroll, J. H., et

476 al. (2009). Evolution of Organic Aerosols in the Atmosphere. *Science*, 326(5959), 1525–

477 1529. <https://doi.org/10.1126/science.1180353>

478 Jo, D. S., Hodzic, A., Emmons, L. K., Tilmes, S., Schwantes, R. H., Mills, M. J., et al. (2021).

479 Future changes in isoprene-epoxydiol-derived secondary organic aerosol (IEPOX SOA)

480 under the Shared Socioeconomic Pathways: the importance of physicochemical

481 dependency. *Atmospheric Chemistry and Physics*, 21(5), 3395–3425.

482 <https://doi.org/10.5194/acp-21-3395-2021>

483 Klein Goldewijk, K., Beusen, A., Doelman, J., & Stehfest, E. (2017). Anthropogenic land use

484 estimates for the Holocene – HYDE 3.2. *Earth System Science Data*, 9(2), 927–953.

485 <https://doi.org/10.5194/essd-9-927-2017>

486 Kloster, S., Mahowald, N. M., Randerson, J. T., Thornton, P. E., Hoffman, F. M., Levis, S., et al.
487 (2010). Fire dynamics during the 20th century simulated by the Community Land Model.
488 *Biogeosciences*, 7(6), 1877–1902. <https://doi.org/10.5194/bg-7-1877-2010>

489 Kloster, S., Mahowald, N. M., Randerson, J. T., & Lawrence, P. J. (2012). The impacts of
490 climate, land use, and demography on fires during the 21st century simulated by CLM-
491 CN. *Biogeosciences*, 9(1), 509–525. <https://doi.org/10.5194/bg-9-509-2012>

492 Lawrence, D. M., Fisher, R. A., Koven, C. D., Oleson, K. W., Swenson, S. C., Bonan, G., et al.
493 (2019). The Community Land Model Version 5: Description of New Features,
494 Benchmarking, and Impact of Forcing Uncertainty. *Journal of Advances in Modeling
495 Earth Systems*, 11(12), 4245–4287. <https://doi.org/10.1029/2018MS001583>

496 Li, F., Zeng, X. D., & Levis, S. (2012). A process-based fire parameterization of intermediate
497 complexity in a Dynamic Global Vegetation Model. *Biogeosciences*, 9(7), 2761–2780.
498 <https://doi.org/10.5194/bg-9-2761-2012>

499 Li, F., Levis, S., & Ward, D. S. (2013). Quantifying the role of fire in the Earth system –
500 Part 1: Improved global fire modeling in the Community Earth System Model (CESM1).
501 *Biogeosciences*, 10(4), 2293–2314. <https://doi.org/10.5194/bg-10-2293-2013>

502 Li, F., Bond-Lamberty, B., & Levis, S. (2014). Quantifying the role of fire in the Earth system –
503 Part 2: Impact on the net carbon balance of global terrestrial ecosystems for the 20th
504 century. *Biogeosciences*, 11(5), 1345–1360. <https://doi.org/10.5194/bg-11-1345-2014>

505 Li, F., & Lawrence, D. M. (2017). Role of Fire in the Global Land Water Budget during the
506 Twentieth Century due to Changing Ecosystems. *Journal of Climate*, 30(6), 1893–1908.
507 <https://doi.org/10.1175/JCLI-D-16-0460.1>

508 Li, F., Lawrence, D. M., & Bond-Lamberty, B. (2018). Human impacts on 20th century fire
509 dynamics and implications for global carbon and water trajectories. *Global and Planetary
510 Change*, 162, 18–27. <https://doi.org/10.1016/j.gloplacha.2018.01.002>

511 Li, F., Val Martin, M., Andreae, M. O., Arneth, A., Hantson, S., Kaiser, J. W., et al. (2019).
512 Historical (1700–2012) global multi-model estimates of the fire emissions from the Fire
513 Modeling Intercomparison Project (FireMIP). *Atmospheric Chemistry and Physics*,
514 19(19), 12545–12567. <https://doi.org/10.5194/acp-19-12545-2019>

515 Li, F., Song, X., Harrison, S. P., Marlon, J. R., Lin, Z., Leung, L. R., et al. (2024). Evaluation of
516 global fire simulations in CMIP6 Earth system models. *Geoscientific Model
517 Development*, 17, 8751–8771. <https://doi.org/10.5194/gmd-17-8751-2024>

518 Liu, X., Ma, P.-L., Wang, H., Tilmes, S., Singh, B., Easter, R. C., et al. (2016). Description and
519 evaluation of a new four-mode version of the Modal Aerosol Module (MAM4) within
520 version 5.3 of the Community Atmosphere Model. *Geoscientific Model Development*,
521 9(2), 505–522. <https://doi.org/10.5194/gmd-9-505-2016>

522 Lu, Z., Liu, X., Ke, Z., Zhang, K., Ma, P.-L., & Fan, J. (2024). Incorporating an interactive fire
523 plume-rise model in the DOE's energy exascale earth system model version 1 (E3SMv1)
524 and examining aerosol radiative effect. *Journal of Advances in Modeling Earth Systems*,
525 16, e2023MS003818. <https://doi.org/10.1029/2023MS003818>

526 Lund, M. T., Rap, A., Myhre, G., Haslerud, A. S., & Samset, B. H. (2021). Land cover change in
527 low-warming scenarios may enhance the climate role of secondary organic aerosols.
528 *Environmental Research Letters*, 16(10), 104031. <https://doi.org/10.1088/1748-9326/ac269a>

530 NCAR. (2023). Community Earth System Model Version 2.2.2 [Software]. Github.
531 <https://github.com/ESCOMP/CESM/releases/tag/cesm2.2.2>

532 Randerson, J. T., van der Werf, G. R., Giglio, L., Collatz, G. J., & Kasibhatla, P. S. (2018).
533 Global Fire Emissions Database, Version 4.1 (GFEDv4). [Dataset]. ORNL
534 DAAC. <https://doi.org/10.3334/ORNLDaac/1293>

535 Riahi, K., van Vuuren, D. P., Kriegler, E., Edmonds, J., O'Neill, B. C., Fujimori, S., et al.
536 (2017). The Shared Socioeconomic Pathways and their energy, land use, and greenhouse
537 gas emissions implications: An overview. *Global Environmental Change*, 42, 153–168.
538 <https://doi.org/10.1016/j.gloenvcha.2016.05.009>

539 Scott, C. E., Monks, S. A., Sprancklen, D. V., Arnold, S. R., Forster, P. M., Rap, A. et al. (2018).
540 Impact on short-lived climate forcers increases projected warming due to deforestation.
541 *Nature Communications*, 9, 157. <https://doi.org/10.1038/s41467-017-02412-4>

542 SEDAC. (2018). Gridded population of the world, version 4 (GPWv3): Population Density,
543 Revision 11 [Dataset]. NASA. <https://doi.org/10.7927/H49C6VHW>

544 Shi, Y., Heald, C. L., Val Martin. (2025). Data from: Future anthropogenic land use change
545 impacts on natural carbonaceous aerosol and implications for climate and air quality
546 [Dataset]. Zenodo. <https://doi.org/10.5281/zenodo.14873517>

547 Sporre, M. K., Blichner, S. M., Karset, I. H. H., Makkonen, R., & Berntsen, T. K. (2019).
548 BVOC-aerosol-climate feedbacks investigated using NorESM. *Atmospheric Chemistry
549 and Physics*, 19, 4763-4782, <https://doi.org/10.5194/acp-19-4763-2019>

550 Tang, W., Emmons, L. K., Buchholz, R. R., Wiedinmyer, C., Schwantes, R. H., He, C., et al.
551 (2022). Effects of fire diurnal variation and plume rise on U.S. air quality during FIREX-
552 AQ and WE-CAN based on the Multi-Scale Infrastructure for Chemistry and Aerosols

553 (MUSICAv0). *Journal of Geophysical Research: Atmospheres*, 127, e2022JD036650.

554 <https://doi.org/10.1029/2022JD036650>

555 Tang, W., Tilmes, S., Lawrence, D. M., Li, F., He, C., Emmons, L. K., et al. (2023). Impact of
556 solar geoengineering on wildfires in the 21st century in CESM2/WACCM6. *Atmospheric*
557 *Chemistry and Physics*, 23(9), 5467–5486. <https://doi.org/10.5194/acp-23-5467-2023>

558 Tilmes, S., Hodzic, A., Emmons, L. K., Mills, M. J., Gettelman, A., Kinnison, D. E., et al.
559 (2019). Climate Forcing and Trends of Organic Aerosols in the Community Earth System
560 Model (CESM2). *Journal of Advances in Modeling Earth Systems*, 11(12), 4323–4351.
561 <https://doi.org/10.1029/2019MS001827>

562 Unger, N. (2014). On the role of plant volatiles in anthropogenic global climate change.
563 *Geophysical Research Letters*, 41(23), 8563–8569.
564 <https://doi.org/10.1002/2014GL061616>

565 Val Martin, M., Logan, J. A., Kahn, R. A., Leung, F.-Y., Nelson, D. L., & Diner, D. J. (2010).
566 Smoke injection heights from fires in North America: analysis of 5 years of satellite
567 observations. *Atmospheric Chemistry and Physics*, 10, 1491–1510.
568 <https://doi.org/10.5194/acp-10-1491-2010>

569 van der Werf, G. R., Randerson, J. T., Giglio, L., Collatz, G. J., Mu, M., Kasibhatla, P. S., et al.
570 (2010). Global fire emissions and the contribution of deforestation, savanna, forest,
571 agricultural, and peat fires (1997–2009). *Atmospheric Chemistry and Physics*, 10(23),
572 11707–11735. <https://doi.org/10.5194/acp-10-11707-2010>

573 van der Werf, G. R., Randerson, J. T., Giglio, L., van Leeuwen, T. T., Chen, Y., Rogers, B. M.,
574 et al. (2017). Global fire emissions estimates during 1997–2016. *Earth System Science
575 Data*, 9(2), 697–720. <https://doi.org/10.5194/essd-9-697-2017>

576 Veira, A., Kloster, S., Schutgens, N. A. J., & Kaiser, J. W. (2015). Fire emission heights in the
577 climate system – Part 2: Impact on transport, black carbon concentrations and radiation.
578 *Atmospheric Chemistry and Physics*, 15, 7173-7193. <https://doi.org/10.5194/acp-15-7173-2015>

580 Ward, D. S., Mahowald, N. M., & Kloster, S. (2014). Potential climate forcing of land use and
581 land cover change. *Atmospheric Chemistry and Physics*, 14(23), 12701–12724.
582 <https://doi.org/10.5194/acp-14-12701-2014>

583 Ward, D. S., & Mahowald, N. M. (2015). Local sources of global climate forcing from different
584 categories of land use activities. *Earth System Dynamic*, 6, 175-194.
585 <https://doi.org/10.5194/esd-6-175-2015>

586 Weber, J., King, J. A., Abraham, N. L., Grosvenor, D. P., Smith, C. J., Shin, Y. M., et al. (2024).
587 Chemistry-albedo feedbacks offset up to a third of forestation's CO₂ removal benefits.
588 *Science*, 383, 860-864. <https://doi.org/10.1126/science.adg6196>

589 WHO. (2021). WHO global air quality guidelines. Geneva, Switzerland: World Health
590 Organization

591 Wiedinmyer, C., Kimura, Y., McDonald-Buller, E. C., Emmons, L. K., Buchholz, R. R., Tang,
592 W., et al. (2023). The Fire Inventory from NCAR version 2.5: an updated global fire
593 emissions model for climate and chemistry applications. *Geoscientific Model
594 Development*, 16(13), 3873–3891. <https://doi.org/10.5194/gmd-16-3873-2023>

595 Wiedinmyer, C., Kimura, Y., McDonald-Buller, E. C., Emmons, L. K., Buchholz, R. R., Tang,
596 W., et al. (2023). Fire Inventory from NCAR version 2 Fire Emission [Dataset].
597 Computational and Information Systems Laboratory. <https://doi.org/10.5065/XNPA-598 AF09>

599 Wu, S., Mickley, L. J., Kaplan, J. O., & Jacob, D. J. (2012). Impacts of changes in land use and
600 land cover on atmospheric chemistry and air quality over the 21st century. *Atmospheric
601 Chemistry and Physics*, 12(3), 1597–1609. <https://doi.org/10.5194/acp-12-1597-2012>

602 Zhang, Q., Jimenez, J. L., Canagaratna, M. R., Allan, J. D., Coe, H., Ulbrich, I., et al. (2007).
603 Ubiquity and dominance of oxygenated species in organic aerosols in anthropogenically-
604 influenced Northern Hemisphere midlatitudes. *Geophysical Research Letters*, 34(13).
605 <https://doi.org/10.1029/2007GL029979>

606